Assessment of low-temperature synthesis of carbon self-doped TiO_2 and its photo catalytic activity under visible light irradiation

Nikoo Moghimi, Manouchehr Nikazar, Hamed Bazrafshan*

Department of Chemical Engineering, Amirkabir University of Technology (Tehran Polytechnic), Tehran, Iran,
email: nikoomoghimi.41@gmail.com (N. Moghimi), nikazar@aut.ac.ir (M. Nikazar),hamed_baz@aut.ac.ir (H. Bazrafshan)

ABSTRACT

Highly efficient carbon self-doped TiO_2 catalysts were obtained using a sol-gel synthesis method, under low-temperature calcination condition and thus a considerable reduction in energy consumption was achieved. Tetrabutyl orthotitanate was utilized as the precursor for both carbon and titanium. Calcination temperatures were chosen between 150 and 400. Methyl Orange decolorization was carried out using the self-doped TiO_2 as well as Degussa-P25 in a slurry batch reactor under visible light irradiation. The results were then compared to investigate the relation between the level of carbon-self doping and the calcination temperature and time. It was observed that the maximum percentage of decolorization occurred at 250 after 2 h. However, it was noticed that under other conditions decolorization was reduced or was even ceased. Assessment of the catalysts characterization was performed by means of XRD, FE-SEM, EDS, DRS and TEM. XRD analysis indicated that the synthesized TiO_2 was crystallized in anatase phase with a crystalline size of 19nm. FE-SEM images illustrate agglomerated spherical shapes around 17–24 nm and the TEM image also validated this results. The reduction of EDS analysis region as well as the value of the energy band gap which was decreased to 3.05 eV confirmed the incorporation of carbon in TiO_2 lattice. According to the results obtained UV-Vis spectrometry, a sudden increase over the range of wavelengths from 450 to 350 nm indicated the visible light photo catalytic activity of $C-TiO_2$ which led to the contaminants becoming decomposed. The photo catalytic decolorization of MO was noticed to obey the Langmuir-Hinshelwood kinetic model. The persistency of $C-TiO_2$ was found to be acceptable as well.

Keywords: Visible light; Low temperature; Carbon-doped; TiO_2; Methyl Orange; Photo catalysts; Sol-gel

1. Introduction

Photo catalysis is known as a "green chemistry" technology; in other words, this technique is not only considered economical but also is environmentally friendly. Due to high oxidative power, photo stability, low cost, and non-toxicity, photo catalysts are the promising candidates in the process of decomposition of organic contaminants in water and also in converting solar energy into chemical energy [1–5].

Due to the advantages derived from both TiO_2 and doped-TiO_2, as photo catalysts, they have recently attracted a great deal of attention in the field of photo degradation. [6–8]. Because of its photochemical stability, non-toxicity, high efficiency and low cost TiO_2 in its anatasie form is among the effective photo catalysts being most widely used and the present study is no exception [9–12]. Typically, high required band gap energy (~3.2 eV) for excitation of semiconductor, affects the efficiency of TiO_2-mediated photo catalytic processes; on the one hand this needs irradiation in the Ultraviolet (UV) range which contains shorter wavelengths and on the other hand, solar radiation at the surface of the earth consists of mainly longer wavelengths, with only 3–5% being UV [13,14]. Recently, researchers have reported that extension of the absorption wavelength from UV to visible region is feasible by doping TiO_2 with

*Corresponding author.

non-metals such as S, B, N, F, Si and C etc. which is related to the localized electronic state in the band gap [15–23]. Formation of the electron (e-) -hole (h+) pairs is the result of irradiation of light with photon energy greater than or equal to the band gap energy of the photo catalyst, consequently these electron (e-) -hole (h+) pairs migrate to the surface and react with the adsorbed species over the surface of photo catalyst to produce the active radicals ($\cdot O_2^-$, $\cdot OH$, h+, etc.) in order to destroy or mineralize different organic contaminants [24]. Doping with nonmetal atoms is more effective than transition metal doping in which poor photo stability of samples was noticed. Moreover, this could prevent the recombination of photo generated e– and h+ or extend the light absorption of TiO_2 into the visible light region [25]. The incorporation of carbon impurities into TiO_2 lattice under controlled condition is a method to induce visible light photo catalytic activity. Although the carbon-doped TiO_2 (C-TiO_2) has been prepared through different synthetic methods, enhancing the adsorption of organic substrates can be achieved using TiO_2-mounted activated carbon and carbon-coated TiO_2. According to the literature, the carbon dopant not only can play the role of an anion which replaces oxygen substitutional in the lattice but also acts as the cation that occupies an interstitial lattice site. The formal oxidation state of carbon dopants has both Ti–C bond as carbides and C–O bond as carbonates. Ti–C bond is formed under conditions such as flame pyrolysis of Ti metal sheet annealing of TiC powders evaporation. However, C–O bond (as carbonate) is often compromised under conditions like sol–gel processes using carbon precursors and high-temperature reactions. Therefore, whether or not being comprised of both states is highly dependent on the preparation method as well as the condition of calcinations [26]. The methods of synthesis include simple mixing of a carbon nano-material with TiO_2, direct oxidation of Ti metal in a burner flame, sol–gel synthesis, hydrothermal synthesis, and deposition techniques such as physical vapor deposition (PVD), chemical vapor deposition (CVD), and electrophoretic deposition, etc. [27,28]. Typically prevailing of three polymorphs, rutile, anatase, and brookite have been confirmed in nature, and anatase titania is usually considered to be more active than rutile crystalline [29]. Various energy-consuming synthesis methods have been applied using temperatures higher than 400; however, in the present study a range of temperatures between 150–400 have been used resulting in a highly efficient C doped TiO_2. This means that the applied method is more economically advantageous regarding time and energy consumption. Furthermore, it was found out that the synergistic effect of low temperature calcination and carbon self-doping is responsible for the improvement of the visible light photo catalytic activity of carbon doped TiO_2 catalyst.

Conventionally when it comes to carbon doping, an external carbon precursor such as glucose needs to be added, while the most attractive feature of the method used in this work is that titanium alkoxide acts as Ti and carbon precursor, simultaneously. In the other words carbon self-doping happens. The nano powder of C-TiO_2 was prepared using the sol-gel method under controlled condition. The effect of time and temperature of calcination on the photo catalytic activity of C-TiO_2 was taken into investigation, so the objective of the recent work was to examine different heat treating temperature and time, in order to find the optimum condition of synthesis. The photo catalytic activity of the catalysts was evaluated by mean of the degradation of methyl orange (MO) as model contaminant. According to the numerous studies conducted on environmental clean-up from such dyes, methyl orange has been commonly used as a model dye. Methyl orange is a dye that is presumed to be mutagenic. It is dissolvable in water and its color varies with pH, from yellow (at pH values higher than 4.4) to red (at lower pH values), so that is why it is known as an indicator. Moreover, methyl orange is an example of the widely used azo dies in textile industry and it is also resistant to biodegradation [30–32]. The micro structures at the nano scale (crystallinity, surface area, crystal phase, and crystal plane) strongly affect the optical absorption properties and catalytic performance of semiconductor photo catalysts [4]. The optimal condition of synthesis was obtained by taking the maximum percentage of decolorization into consideration through investigating different calcination temperature and time. subsequently the study continued by preparing the catalyst in the optimal condition to proof this claim that the decolorization percentage is adequate. X-ray powder diffraction (XRD), Field Emission Scanning Electron Microscopy (FE-SEM), Transmission electron microscopy (TEM), X-ray spectroscopy (EDS), and Diffuse Reflectance Spectra (DRS) and UV–Vis spectrometer were utilize to characterize the carbon-doped TiO_2. Furthermore, in order to study the influential factors which could affect the experiments and enhance the visible light photo catalytic properties of the optimal prepared catalyst, factors such as initial dye concentration, catalytic dose, and pH were also taken into consideration. All the photo catalytic experiments using the prepared catalysts indicated higher performance compared with Degussa-P25 which can be attributed to visible light photo catalytic activity of the carbon self-doped TiO_2. The authors definitely recommend considering the present approach in future studies as it is helpful in preparation of a highly stable TiO_2-based photo catalyst which could also become active under visible irradiation.

2. Materials and methods

2.1. Preparation of TiO₂ photo catalyst

All chemicals are analytical-reagent grade, used directly without any further purification. Deionized water, tetrabutyl orthotitanate, ethanol and $HClO_4$ were used to synthesize the photo catalysts. For this purpose, the sol-gel was prepared as follows: 11 mL of tetrabutyl orthotitanate was dissolved in 50 mL of ethanol under vigorous magnetic stirring for 30 min; in the meantime, $HClO_4$ solution (0.5 mL) was dropped into solution gently. Afterwards, the obtained solution was sealed and then stirring continued for another 30 min, the resulting gel was aged for 2 d, at room temperature and was later dried in an oven at 100°C for 1 d. Finally, powder was heat-treated in a furnace at various temperature and time according to Table 1.

2.2. Characterization

The crystal structure of the samples were characterized using X-ray powder diffraction (XRD) using Cu-Kα radi-

Table 1
Selected condition for as-prepared catalysts

Number of experiment	Calcination temperature	Time of calcination (h)	MO Removal (%)
1	150	0.5	14
2	150	2	31
3	150	3	40
4	250	0.5	19
5	250	2	59
6	250	3	45
7	400	0.5	20
8	400	2	7
9	400	3	3

ation (Equinox 3000, Inel France). Both TiO_2 surface morphology and the size of particles were studied using Field Emission Scanning Electron Microscopy (FE-SEM, Leo 1450 VP, Zeies, Germany) and Transmission electron microscopy (TEM, EM900, Zeies, Germany). Typically, the percentage of carbon doping is shown by Energy Dispersive X-ray spectroscopy (EDS, Axford, England) and the diffuse reflectance spectra (DRS). The photo catalytic performance was characterized using UV-Vis spectrometer (Avantes Avaspec-2048-TEC, Russian).

2.3. Photo catalytic activity test

A slurry photochemical reactor, as shown in Fig. 1 was set up, to evaluate the photo catalytic activity of the catalyst through methyl orange (MO ($C_{14}H_{14}N_3NaO_3S$)) degradation; to prevent the effects of external irradiating, an aluminum cover was used to stop outside light from entering the reactor and then visible light (> 400 nm) was illuminated inside the reactor, through the experiments. Before the light irradiation, 0.05 g of photo catalyst was added to 50 mL MO aqueous solution (pH = 4.5), the mixture was then kept in the dark for 1 h applying magnetic stirring so that the solution would reach the adsorption–desorption equilibrium. The light source was a 16 W visible light. To ensure that enough oxygen could reach the reaction suspension, the solution was bubbled with air during irradiation using a gas flow rate of 0.25 l/min. At certain time intervals, 3 mL aliquots were sampled and centrifuged to remove the nano-particles, and finally the filtrates were analyzed by recording variations of absorbency at the maximum absorption band (460 nm for MO) using a UV-visible spectrophotometer (Cecil CE 2501, England).

3. Results and discussion

3.1. Visible light photo catalytic activity

Some experiments were conducted in the slurry-batch reactor to determine the visible light photo catalytic activities of the as-prepared TiO_2 catalysts, by means of decolorization of MO solutions (under the mentioned condition in part 2.3). The highest MO removal percentage under
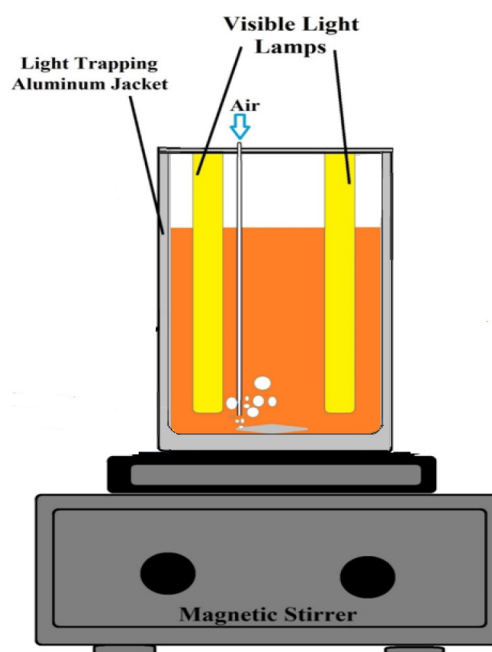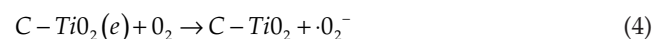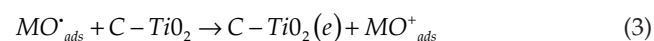

Fig. 1. Schematic representation of photo catalytic reactor.

even condition was found to occur at the catalyst dosage of 0.001 g/mL, initial MO concentration of 30 mg/L, and the pH of 4.5; additionally, the pH of the suspension was adjusted with $HClO_4$ or NaOH standard solution. No decolorization of MO was observed in the absence of a photo catalyst under visible light illumination. The concentration of MO was calculated using a calibration curve which was also compared with the results achieved for P-25. Moreover, the percentage of dye removal was calculated as given by Eq. (1):

$$\%\text{Color Removal} = \left(\frac{C_0 - C_t}{C_0} \right) \times 100 \qquad (1)$$

where C_0 is the initial concentration of dye in mg/L and C_t is dye concentration in mg/L at any time t.

The chemical mechanism of photo sensitization of the catalyst by methylene Orange is shown in the following equations, which could occur for both P25 and C-TiO_2 as MO is directly excited by long-wavelength light:

$$MO_{ads} + visible light \rightarrow MO^{\cdot} ads \qquad (2)$$

$$MO^{\cdot}_{ads} + C - TiO_2 \rightarrow C - TiO_2(e) + MO^+_{ads} \qquad (3)$$

$$C - TiO_2(e) + O_2 \rightarrow C - TiO_2 + \cdot O_2^- \qquad (4)$$

where *ads* is the abbreviation of 'adsorbed' and conveys adsorbed state of species. In addition, Eqs. (2)–(4) convey that the adsorbed MO is excited by visible light and an electron from the excited dye may be injected to the conduction band of the catalyst, where the molecular oxygen has occupied it. However, the direct excitation of the semiconductor can occur at lower wavelengths according to the following reactions:

$$C - TiO_2 + visible\ light \rightarrow h^+ + e^- \tag{5}$$

$$e^- + O_2 \rightarrow \cdot O^{2-} \tag{6}$$

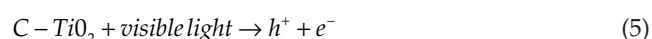$$h^+ + H_2O \rightarrow \cdot OH \tag{7}$$

Fig. 2 serves to show a pictorial illustration of these processes. Decolorization of the solution through a photo catalytic mechanism could be facilitated using direct excitation of the powders by lower wavelength of light as the visible light absorbance of the carbon doped samples were improved due to the reduced band gap compared to P25. Since as was mentioned in previous literatures, P25 could only be excited using a UV source, the improvement of photo catalytic activity and reduction of the band gap could be attributed to the presence of interface states and/or interface defects caused by carbon doping [33].

According to the mentioned equations the active species generated in the photo catalytic process are different such as electrons, holes, ·OH, ·O²⁻, etc., so these sacrificial reagents play an important role in the photo catalytic reaction. Organic species are quickly oxidized at the surface of TiO₂ particles by highly reactive ·O²⁻ and ·OH radicals which are produced from the reaction between photo generated-holes and electrons with surface hydroxyl groups or adsorbed water or O_2 [34,35].

The kinetic of the photo catalytic decolorization may be evaluated as follows:

$$ln\left(\frac{C_0}{C}\right) = kt \tag{8}$$

where k is a constant rate of reaction, C_0 and C are initial and final concentration of methyl orange. It was observed that the photo catalytic decolorization of MO was a pseudo-first order reaction according to Langmuir-Hinshelwood model.

It was also noticed that the efficiency of MO photo degradation and visible light photo catalytic activity for all the as-prepared TiO₂ samples were higher than that of P-25 as illustrated in Fig. 3. The TiO₂ nano particles at the heat-treating time of 2 h and heat-treating temperature of 250 showed the best visible light photo catalytic activity. Finally, to make a comparison between different as-prepared catalysts char-
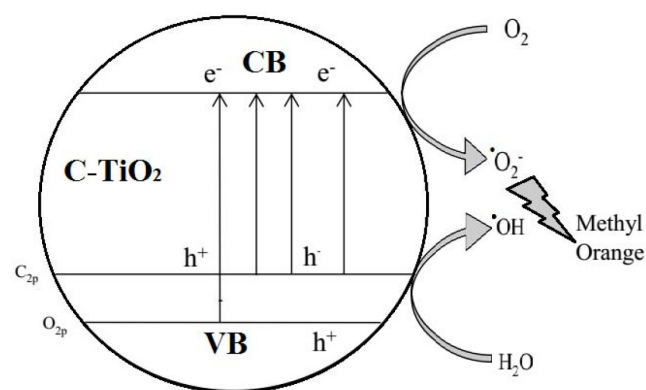
acterization, the samples with the highest decolorization percentage in each set of experiments were chosen; such as TiO₂ (150, 0.5 h), TiO₂(250, 2 h), TiO₂ (400, 0.5 h) samples.

3.2. Characterization of C-doped TiO₂

Fig. 4 shows the XRD patterns of the TiO₂ photo catalysts prepared under the mentioned condition, the X-ray diffraction adopts Cu Kα (λ = 1.54065A°) radiation within the 2 = 10–90° region, additionally the grain or the crystalline size (L) of anatase TiO₂ can be calculated from the line broadening by Scherrer's formula as Eq. (7):

$$L = \frac{k\lambda}{\beta Cos\theta} \tag{9}$$

where L represents crystallite size of pure TiO₂ (nm), k is a dimensionless shape factor (= 0.94), λ is the wavelength of X-ray (Cu Kα = 0.154065 nm), is line broadening at half the maximum intensity, and is the half diffraction
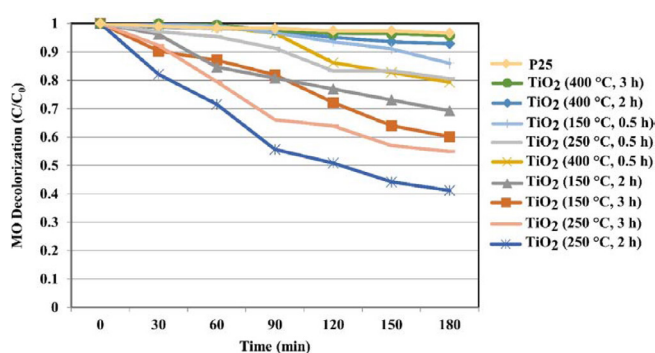

Fig. 3. Effect of catalyst preparation condition on dye decolorization; concentration of MO: 30 mg/L, catalyst dosage: 0. 001 g/mL; pH: 4.5; temperature 32 ± 2°C; time: 3 h.

Fig. 2. Possible mechanism for the photo catalytic activity of C-TiO₂ samples to methyl orange degradation.
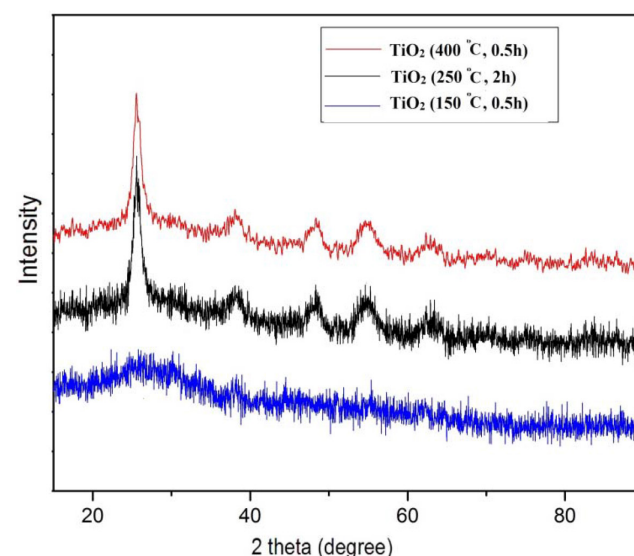

Fig. 4. XRD patterns of three samples of as-prepared TiO₂ photo catalysts.

angle of 2 in degree [36,37]. The Crystalline size of the doped TiO_2 (250, 2h) was calculated 19 nm, according to the XRD picks in Fig. 4 and as was compared with other references the produced phase after calcination is anatas, increasing the temperature to 250 causes the increasing in crystallinity of $C-TiO_2$ [38]. The Brunauer–Emmett–Teller (BET) surface area measurements were performed with nitrogen as an adsorptive gas, according to the surface area of the samples TiO_2 (250, 2 h), TiO_2 (150, 0.5 h), and TiO_2 (400, 0.5 h) was 57, 79, and 49 m^2/g respectively this variation was due to the different calcination time and temperature [39,40].

The morphology of the three samples is depicted in Fig. 5, one can find that the morphology of $C-TiO_2$(150°C, 0.5 h) and $C-TiO_2$(250°C, 2 h) are similar to each other but the $C-TiO_2$(400°C, 0.5 h) is different from those related to the nearly high calcination temperature and the results show that the second sample has a fine agglomerated spherical shape around 24–40 nm, it means the size of nano particles

will be 1.5–2 times more than that of the size approved by Scherrer's formula, besides TEM image in Fig. 5c reveals the diameters of approximately 24–40 nm for produced nano powders . Fig. 5b also shows the percent of carbon, titanium, and oxygen in the EDS analysis region, the EDS confirms the carbon existence in $C-TiO_2$(150°C, 0.5 h) and $C-TiO_2$(250°C, 2 h), but the largest amount of doped carbon among catalysts belongs to 250°C, 2 h calcination condition according to Fig. 5b. The un-labeled picks are related to Au and palladium that are used for the coating of powder in FE-SEM apparatus.

The optical absorption and band gap energy of C-doped TiO_2 catalysts prepared under the condition of 250 and 2 h, as the optimum sample, were measured by spectrophotometer within a wavelength range of 300–900 nm by means of DRS and was compared with the DRS of the sample with no carbon; TiO_2(400°C , 0.5 h), as shown in Fig. 6. According to the spectrum a sudden increase in the region between 450 nm and 350 nm could be related to the band gap absorp-
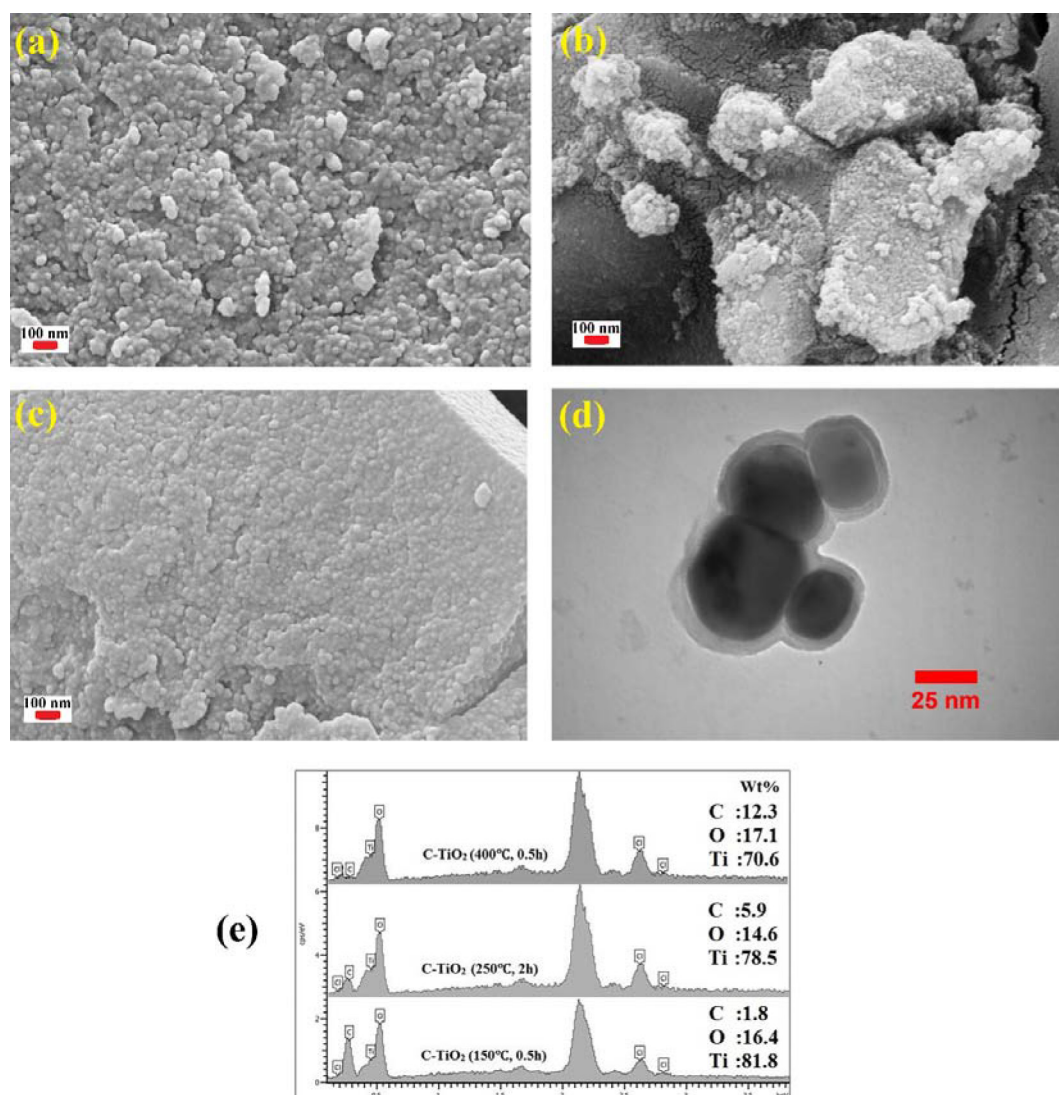

Fig. 5. FE-SEM images of (a) TiO_2 (150°C, 0.5 h) (b) TiO_2 (400°C, 0.5 h) (c) TiO_2 (250°C, 2 h), (d) TEM image of TiO_2 (250°C, 2 h) (e) EDS elemental analyses of prepared TiO_2.
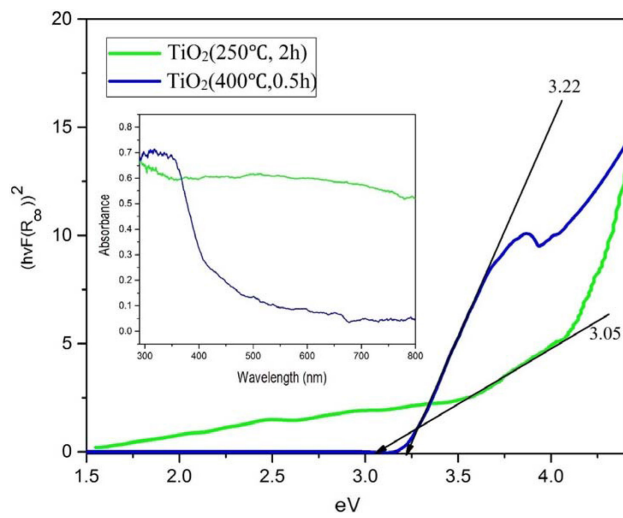
Fig. 6. Optical band gap energy of TiO$_2$ (250°C, 2 h) and TiO$_2$ (400°C, 0.5 h) (Inset: UV-Vis DRS absorption spectra of the samples).

tion of TiO$_2$. The following equations are applicable to estimation of band gap energy (E_g) by using Kubelka-Munk function [41,42]:

$$F(R_\infty) = \frac{(1-R_\infty)^2}{2\,R_\infty} \qquad (10)$$

$$(h\nu\alpha)^2 = C(h\nu - E_g) \qquad (11)$$

$$\alpha \propto F(R_\infty) \qquad (12)$$

F (R∞) is the Kubelka-Munk function, *R* is the reflectance of an infinitesimal thick sample, α is absorption coefficient, *hν* is the photon energy, *C* is a constant, and E_g is the band gap energy of material C-TiO$_2$.

The band gap energy was calculated applying (F(R$_\infty$) hν)^2 versus (hν) area that is given in Fig. 5. The evaluated energy band gap value in TiO$_2$ (250°C, 2 h) was close to 3.05 eV which was smaller than TiO$_2$ (400°C, 0.5 h) with the band gap energy of 3.22 eV. This decrease in E_g can be attributed to the effect of the carbon self-doping [43].

3.3. Visible light photo catalytic properties

In order to verify the visible light photo catalytic activity of the chosen catalyst, TiO$_2$ (250°C, 2 h), further experiments were conducted using the slurry-batch reactor and the impact of the three parameters, initial dye concentration, catalytic dosage, and pH was investigated. The decolorization percentage of MO (20 mg/L) versus catalytic doses is plotted in Fig. 7a. The decolorization percentage was increased up to a dosage of 1 g/L and was remained almost constant up to a dosage of 2 g/L. Then, it was decreased slowly at higher catalyst doses. The decline of the decolorization can be related to accumulation of catalyst particles which could lead to the solution become opaque and light scattering of TiO$_2$ particles at high concentration could also
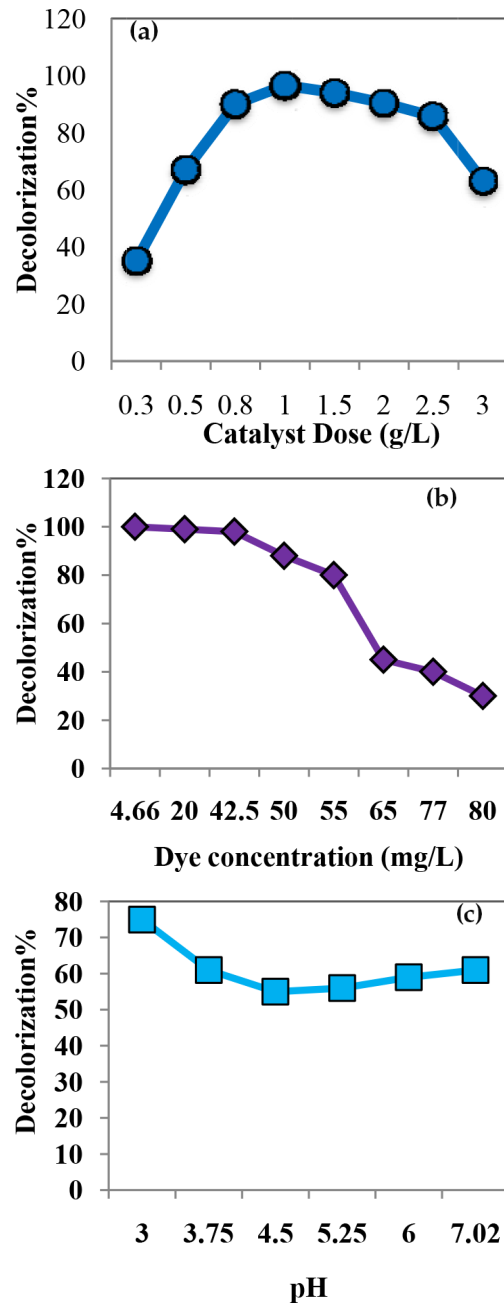

Fig. 7. (a) Effect of catalytic dosage on dye decolorization; concentration of MO: 20 mg/L; pH: 4; temperature: 32 ± 2 ; time: 1 h. (b) Effect of initial dye concentration on dye decolorization; C doped TiO$_2$: 1 g/L; PH: 4; temperature: 32 ± 2°C; time: 1 h. (c) Effect of pH of reaction mixture on dye decolorization; C doped TiO$_2$: 1 g/L; concentration of MO: 20 mg/L; temperature: 32 ± 2 °C; time: 1 h.

increase. On the other hand, absorption of dye molecules could decrease as a result of reduction in the number of catalyst surface active sites [44].

The next key parameter taken into account was initial concentration, and its effect on the decolorization percentage of MO was then investigated as presented in Fig. 7b. As the initial concentration grew the decolorization

rate decreased, due to the fact that the rate of production of oxidants falls and catalyst surface active sites reduces [43,45].

A pH range 3–7 was considered according to Fig. 7c. With a look at the diagram, one sees that the decolorization percentage is higher in acidic medium, and slightly reduces moving to the higher pH values. The amphoteric behavior of most semiconductor oxides affects the surface charge of photo catalyst, so the variation in the decolorization percentage at different pH values can be attributed to the pH value of zero-point charge (pH_{zpc}) of TiO_2. The pH_{zpc} of TiO_2 particles was around 6 as Ti_{IV}-OH, in other words, when the pH level was lower than 6, the adsorbent surface became positively charged, Ti_{IV}-OH_2^+, so it could attract anions. On the contrary, when the pH was set above the pH_{zpc} the catalyst surface started repelling anions as it became negatively charged as Ti_{IV}-O_2^- [46]. The MO chemical species and complex species are anion in the solution, therefore, in the pH range of 3–6 photo catalyst degradation of MO accelerated and in the pH range of 6–7 it gradually decreased. The appropriate values of the variables in order to achieve maximum photo catalytic removal of MO was found by a correlation between the variables and the maximum percentage of decolorization. The result showed a a maximum removal of 91% at 0.0009 g/mL, 20 mg/L, and 3.0 of catalytic dose, initial MO concentration, and pH respectively.

3.7. Validation experiment

Validation of the preceding experiments was performed by conducting the photo catalytic degradation of MO under the optimum condition in the slurry-batch reactor. The decolorization percentage was found to be 91% which shows acceptable agreement with the experimental results. Furthermore, the reaction kinetics for the selected optimized condition was studied and the results revealed that the degradation follows the pseudo-first order kinetic model. As shown in Fig. 8a, correlation coefficient R^2 is near 1 and the pseudo-first order rate constant (k) is 0.014 1/min.

3.8. Photo catalytic stability

The Photo catalytic process is partial to the environment as no produced waste is expected, so the demands of environment should be considered. To examine the photo catalytic stability, TiO_2 (250°C, 2 h) was chosen to carry out the recycling experiments. For attaining adsorption/desorption equilibrium. The suspension was magnetically stirred for 60 min in the dark prior to light illumination. According to Fig. 4 no degradation is noticed through this step. Then during light illumination the reaction mixture was sampled at given time intervals. After centrifugation the dye concentration was measured on a UV-vis spectrophotometer The regeneration of the TiO_2 photo catalyst in the recycling experiments was conducted by means of suspension filtration in order to remove the bulk solution. Then drying at 100°C for 10 h was done. Finally, the regenerated TiO_2 was reused for additional photo catalytic experiments. This process was repeated three times (Fig. 8b) [38].

4. Conclusions

In the present study nano carbon-doped TiO_2 was successfully synthesized appling a typical sol-gel process and without using any external carbon precursors through the controlled calcination temperature and time. The visible light activity of C-TiO_2 was observed to be sensitively influenced by the calcination temperature and time in a volcano-shape manner thus increasing the calcination temperature and time resulted in enhanced visible light photo catalytic activity and then the feature gradually disappeared so the best photo catalytic activity was obtained at calcination temperature of 250 and calcination time of 2 h. This could be associated with carbon doping of the catalysts which improves the decomposition of organic contaminant under visible light. The visible light photo catalytic activity of the as-prepared TiO_2 was quantified by means of degradation of MO was found to be greatly higher than the commercial TiO_2 (P-25). Moreover, the photo catalytic stability proved to remain excellent after 7 times regeneration of the catalyst. The catalyst characterization was confirmed by
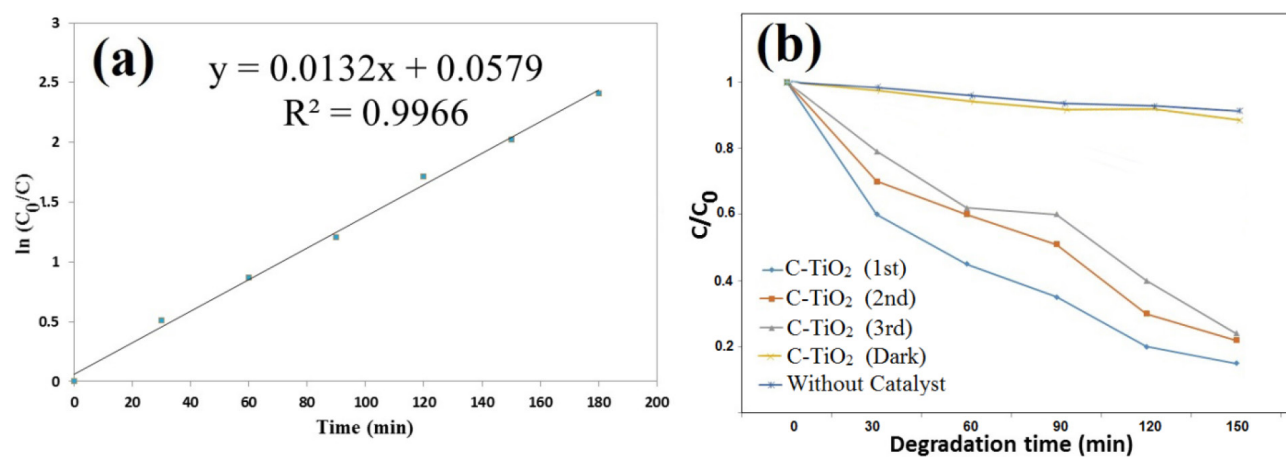

Fig. 8. (a) Evaluation of the rate constants (k) for C-doped TiO_2 selected optimized condition. (b) Result of recycling experiment for C-TiO_2 (250°C, 2 h).

XRD, FE-SEM, TEM, EDS and UV-Vis DRS. Dye decolorization was predicted to be 91% under optimum condition of 0.0009 g/mL of catalyst dose, 20 mg/L of initial dye concentration and the pH of 3. The present energy-efficient method is not only worthwhile economically, but also engenders the reduction of environmental pollution.

References

[1] X. Liu, W. Di, W. Qin, Cooperative luminescence mediated near infrared photo catalysis of CaF_2: Yb@ $BiVO_4$ composites, App. Catal., B 205 (2017) 158–164.

[2] C. Yu, C.Y. Jimmy, A simple way to prepare C–N-codoped TiO_2 photo catalyst with visible-light activity, Catal. Lett., 129(3–4) (2009) 462.

[3] C. Yu, L. Wei, W. Zhou, D.D. Dionysiou, L. Zhu, Q. Shu, H. Liu, A visible-light-driven core-shell like Ag_2S@ Ag_2CO_3 composite photo catalyst with high performance in pollutants degradation, Chemosphere, 157 (2016) 250–261.

[4] C. Yu, W. Zhou, H. Liu, Y. Liu, D.D. Dionysiou, Design and fabrication of micro sphere photo catalysts for environmental purification and energy conversion, Chem. Eng. J., 287 (2016) 117–129.

[5] C. Yu, W. Zhou, L. Zhu, G. Li, K. Yang, R. Jin, Integrating plasmonic Au nano rods with dendritic like α-Bi_2O_3/$Bi_2O_2CO_3$ heterostructures for superior visible-light-driven photo catalysis, App. Cata. B: Envir., 184 (2016) 1–11.

[6] S.-C. Jung, N. Imaishi, Preparation, crystal structure, and photo catalytic activity of TiO_2 films by chemical vapor deposition, Kor. J. Chem. Eng., 18(6) (2001) 867–872.

[7] W.X. Xianyu, M.K. Park, W.I. Lee, Thickness effect in the photo catalytic activity of TiO_2 thin films derived from sol-gel process, Kor. J. Chem. Eng., 18(6) (2001) 903–907.

[8] S.S. Lee, H.J. Kim, K.T. Jung, H.S. Kim, Y.G. Shul, Photo catalytic activity of metal ion (Fe or W) doped Titania, Korean J. Chem. Engng., 18(6) (2001) 914–918.

[9] H. Yu, X. Zheng, Z. Yin, F. Tag, B. Fang, K. Hou, Preparation of nitrogen-doped TiO_2 nano particle catalyst and its catalytic activity under visible light, Chin. J. Chem. Eng., 15(6) (2007) 802–807.

[10] W. Zhuang, L. Lu, W. Li, R. An, X. Feng, X. Wu, Y. Zhu, X. Lu, In-situ synthesized mesoporous TiO_2-B/anatase micro particles: Improved anodes for lithium ion batteries, Chin. J. Chem. Eng., 23(3) (2015) 583–589.

[11] Y. Liu, S. Zhou, F. Yang, H. Qin, Y. Kong, Degradation of phenol in industrial wastewater over the F–Fe/TiO_2 photo catalysts under visible light illumination, Chin. J. Chem. Eng., 24(12) (2016) 1712–1718.

[12] S. Zhang, L. Li, Y. Liu, Q. Zhang, TiO_2–SA–Arg nano particles stabilized pickering emulsion for photo catalytic degradation of nitrobenzene in a rotating annular reactor, Chin. J. Chem. Eng., 25(2) (2017) 223–231.

[13] J.G. McEvoy, W. Cui, Z. Zhang, Degradative and disinfective properties of carbon-doped anatase–rutile TiO_2 mixtures under visible light irradiation, Catal. Today, 207 (2013) 191–199.

[14] M. Safari, M. Nikazar, M. Dadvar, Photo catalytic degradation of methyl tert-butyl ether (MTBE) by Fe-TiO_2 nano particles, Ind. Eng. Chem. Res., 19(5) (2013) 1697–1702.

[15] H. Slimen, H. Lachheb, S. Qourzal, A. Assabbane, A. Houas, The effect of calcination atmosphere on the structure and photo activity of TiO_2 synthesized through an unconventional doping using activated carbon, J. Environ. Chem. Eng., 3(2) (2015) 922–929.

[16] N. Aman, N.N. Das, T. Mishra, Effect of N-doping on visible light activity of TiO_2–SiO_2 mixed oxide photo catalysts, J. Environ. Chem. Eng., 4(1) (2016) 191–196.

[17] V.S. Protsenko, E.A. Vasil'eva, A.V. Tsurkan, A.A. Kityk, S.A. Korniy, F.I. Danilov, Fe/TiO_2 composite coatings modified by ceria layer: Electrochemical synthesis using environmentally friendly methane sulfonate electrolytes and application as photo catalysts for organic dyes degradation, J. Environ. Chem. Eng., 5(1) (2017) 136–146.

[18] N.T. Thao, D.T.H. Ly, H.T.P. Nga, D.M. Hoan, Oxidative removal of rhodamine B over Ti-doped layered zinc hydroxide catalysts, J. Environ. Chem. Eng., 4(4, Part A) (2016) 4012–4020.

[19] M. Pazoki, M. Parsa, R. Farhadpour, Removal of the hormones dexamethasone (DXM) by Ag doped on TiO_2 photo catalysis, J. Environ. Chem. Eng., 4(4, Part A) (2016) 4426–4434.

[20] M. Sanchez-Dominguez, G. Morales-Mendoza, M.J. Rodriguez-Vargas, C.C. Ibarra-Malo, A.A. Rodriguez-Rodriguez, A.V. Vela-Gonzalez, S.A. Perez-Garcia, R. Gomez, Synthesis of Zn-doped TiO_2 nano particles by the novel oil-in-water (O/W) micro emulsion method and their use for the photo catalytic degradation of phenol, J. Environ. Chem. Eng., 3(4, Part B) (2015) 3037–3047.

[21] V. Bhatia, A. Dhir, Transition metal doped TiO_2 mediated photo catalytic degradation of anti-inflammatory drug under solar irradiations, J. Environ. Chem. Eng., 4(1) (2016) 1267–1273.

[22] C. Yu, G. Li, S. Kumar, H. Kawasaki, R. Jin, Stable Au25 (SR) 18/TiO_2 composite nano structure with enhanced visible light photo catalytic activity, Phys. Chem. Lett., 4(17) (2013) 2847–2852.

[23] C. Yu, D. Cai, K. Yang, C.Y. Jimmy, Y. Zhou, C. Fan, Sol–gel derived S, I-codoped mesoporous TiO_2 photo catalyst with high visible-light photo catalytic activity, J. Phys. Chem. Solids, 71(9) (2010) 1337–1343.

[24] C. Yu, Z. Wu, R. Liu, D.D. Dionysiou, K. Yang, C. Wang, H. Liu, Novel fluorinated Bi_2MoO_6 nano crystals for efficient photo catalytic removal of water organic pollutants under different light source illumination, Appl. Catal., B 209 (2017) 1–11.

[25] C. Di Valentin, G. Pacchioni, A. Selloni, Theory of carbon doping of titanium dioxide, Chem. Mater., 17(26) (2005) 6656–6665.

[26] Y. Park, W. Kim, H. Park, T. Tachikawa, T. Majima, W. Choi, Carbon-doped TiO_2 photo catalyst synthesized without using an external carbon precursor and the visible light activity, Appl. Catal., B, 91(1) (2009) 355–361.

[27] H. Bazrafshan, Z.A. Tesieh, S. Dabirnia, A. Naderifar, Low temperature synthesis of TiO_2 nano particles with high photo catalytic activity and photo electrochemical properties through sol–gel method, Mater. Manuf. Process, 31(2) (2016) 119–125.

[28] C.-X. Xu, K.-J. Huang, Y. Fan, Z.-W. Wu, J. Li, Electrochemical determination of acetaminophen based on TiO_2–graphene/poly(methyl red) composite film modified electrode, J. Mol. Liq., 165 (2012) 32–37.

[29] S. Yin, H. Hasegawa, D. Maeda, M. Ishitsuka, T. Sato, Synthesis of visible-light-active nano size rutile titania photo catalyst by low temperature dissolution–reprecipitation process, J. Photo chem. Photobiol., A, 163(1) (2004) 1–8.

[30] H. Mahmoodian, O. Moradi, B. Shariatzadeha, T.A. Salehf, I. Tyagi, A. Maity, M. Asif, V.K. Gupta, Enhanced removal of methyl orange from aqueous solutions by poly HEMA–chitosan-MWCNT nano-composite, J. Mol. Liq., 202 (2015) 189–198.

[31] T. Varadavenkatesan, R. Selvaraj, R. Vinayagam, Phyto-synthesis of silver nano particles from Mussaenda erythrophylla leaf extract and their application in catalytic degradation of methyl orange dye, J. Mol. Liq., 221 (2016) 1063–1070.

[32] P. Mokhtari, M. Ghaedi, K. Dashtian, M.R. Rahimi, M.K. Purkait, Removal of methyl orange by copper sulfide nano particles loaded activated carbon: Kinetic and isotherm investigation, J. Mol. Liq., 219 (2016) 299–305.

[33] C. Yu, L. Wei, J. Chen, Y. Xie, W. Zhou, Q. Fan, Enhancing the photo catalytic performance of commercial TiO_2 crystals by coupling with trace narrow-band-gap Ag_2CO_3, Ind. Eng. Chem. Res., 53(14) (2014) 5759–5766.

[34] W. Li, D. Li, J. Wang, Y. Shao, J. You, F. Teng, Exploration of the active species in the photo catalytic degradation of methyl orange under UV light irradiation, J. Mol. Catal. A: Chem., 380 (2013) 10–17.

[35] Y. Lin, D. Li, J. Hu, G. Xiao, J. Wang, W. Li, X. Fu, Highly efficient photo catalytic degradation of organic pollutants by PANI-modified TiO_2 composite, J. Phys. Chem., C, 116(9) (2012) 5764–5772.

[36] E. Haritha, S.M. Roopan, G. Madhavi, G. Elango, P. Arunachalam, Catunaregum spinosa capped Ag NPs and its photo catalytic application against amaranth toxic azo dye, J. Mol. Liq., 225 (2017) 531–535.

[37] A. S, S. M, [EMIM] BF4 ionic liquid-mediated synthesis of TiO_2 nano particles using Vitex negundo Linn extract and its antibacterial activity, J. Mol. Liq., 221 (2016) 986–992.

[38] W. Desong, X. Libin, L. Qingzhi, L. Xueyan, A. Jing, D. Yandong, Highly efficient visible light TiO_2 photo catalyst prepared by sol-gel method at temperatures lower than 300°C, J. Hazard. Mater., 192(1) (2011) 150–159.

[39] D. Wang, L. Xiao, Q. Luo, X. Li, J. An, Y. Duan, Highly efficient visible light TiO_2 photo catalyst prepared by sol–gel method at temperatures lower than 300°C, J. Hazard. Mater., 192(1) (2011) 150–159.

[40] Y. Park, W. Kim, H. Park, T. Tachikawa, T. Majima, W. Choi, Carbon-doped TiO_2 photo catalyst synthesized without using an external carbon precursor and the visible light activity, Appl. Catal., B, 91(1–2) (2009) 355–361.

[41] I.M. Ibrahim, M.E. Moustafa, M.R. Abdelhamid, Effect of organic acids precursors on the morphology and size of ZrO_2 nano particles for photo catalytic degradation of Orange G dye from aqueous solutions, J. Mol. Liq., 223 (2016) 741–748.

[42] H. Bazrafshan, Z.A. Tesieh, S. Dabirnia, R.S. Touba, H. Manghabati, B. Nasernejad, Synthesis of novel α-Fe_2O_3 nano rods without surfactant and its electrochemical performance, Powder Technol., 308 (2017) 266–272.

[43] H.I. De Lasa, B. Serrano, M. Salaices, Photo catalytic reaction engineering, Springer 2005.

[44] M.R. Sohrabi, M. Ghavami, Photo catalytic degradation of Direct Red 23 dye using UV/TiO_2: Effect of operational parameters, J. Hazard. Mater., 153(3) (2008) 1235–1239.

[45] S. Ahmed, M.G. Rasul, R. Brown, M.A. Hashib, Influence of parameters on the heterogeneous photo catalytic degradation of pesticides and phenolic contaminants in wastewater: A short review, J. Environ. Manage., 92(3) (2011) 311–330.

[46] T. Sugiyama, A.H. Dabwan, H. Katsumata, T. Suzuki, S. Kaneco, Optimization of conditions for the photo catalytic degradation of EDTA in aqueous solution with Fe-doped titanium dioxide, Open J. Inor. Non-meta. Mat., 4(3) (2014) 28.